Adaptive responses to *mTOR* gene targeting in hematopoietic stem cells reveal a proliferative mechanism evasive to mTOR inhibition

Cuiqing Fan[a,b], Chuntao Zhao[a], Feng Zhang[a], Meenu Kesarwani[a,c], Zhaowei Tu[a], Xiongwei Cai[a], Ashley Kuenzi Davis[a], Lingli Xu[a], Cindy L. Hochstetler[a], Xiaoyi Chen[a], Fukun Guo[a], Gang Huang[a,c], Mohammad Azam[a,c], Weidong Tian[a], Q. Richard Lu[a], and Yi Zheng[a,1]

[a]Division of Experimental Hematology and Cancer Biology, Cancer and Blood Diseases Institute, Cincinnati Children's Hospital Medical Center, Cincinnati, OH 45229; [b]Institute of Pediatrics, Children's Hospital of Fudan University, 201102 Shanghai, China; and [c]Division of Pathology, Cancer and Blood Diseases Institute, Cincinnati Children's Hospital Medical Center, Cincinnati, OH 45229

Edited by Brian J. Druker, Oregon Health & Science University, Portland, OR, and approved November 11, 2020 (received for review October 7, 2020)

The mechanistic target of rapamycin (mTOR) is a central regulator of cell growth and an attractive anticancer target that integrates diverse signals to control cell proliferation. Previous studies using mTOR inhibitors have shown that mTOR targeting suppresses gene expression and cell proliferation. To date, however, mTOR-targeted therapies in cancer have seen limited efficacy, and one key issue is related to the development of evasive resistance. In this manuscript, through the use of a gene targeting mouse model, we have found that inducible deletion of *mTOR* in hematopoietic stem cells (HSCs) results in a loss of quiescence and increased proliferation. Adaptive to the *mTOR* loss, *mTOR*$^{-/-}$ HSCs increase chromatin accessibility and activate global gene expression, contrary to the effects of short-term inhibition by mTOR inhibitors. Mechanistically, such genomic changes are due to a rewiring and adaptive activation of the ERK/MNK/eIF4E signaling pathway that enhances the protein translation of RNA polymerase II, which in turn leads to increased *c-Myc* gene expression, allowing the HSCs to thrive despite the loss of a functional mTOR pathway. This adaptive mechanism can also be utilized by leukemia cells undergoing long-term mTOR inhibitor treatment to confer resistance to mTOR drug targeting. The resistance can be counteracted by MNK, CDK9, or c-Myc inhibition. These results provide insights into the physiological role of mTOR in mammalian stem cell regulation and implicate a mechanism of evasive resistance in the context of mTOR targeting.

mTOR | adaptive compensation | drug resistance | hematopoietic stem cells | leukemia

Hematopoietic stem cells (HSCs) are rare cells in the bone marrow (BM) characterized by multilineage differentiation and self-renewal capabilities that ensure lifelong hematopoiesis in mammals (1, 2). HSCs reside in the BM niche and exhibit low cell cycle activity under homeostatic conditions, whereas, under stress, HSCs can increase proliferation and then differentiate to replenish blood cells (3, 4). Disturbance of HSC homeostasis can lead to HSC exhaustion, BM failure, or malignant transformation (5–7); thus, HSC quiescence and proliferation need to be precisely balanced. This process is finely regulated by numerous intrinsic and extrinsic factors and molecular pathways, including metabolic and nutrient-sensing pathways through LKB1 and mTOR signaling (8–11).

mTOR is a serine/threonine kinase that senses and integrates multiple environmental and intracellular signals from nutrients, growth factors, and cellular energy status to regulate protein synthesis, autophagy, metabolism, cell survival, cell growth, and proliferation (12). Growing evidence has established an essential role for mTOR in regulating hematopoiesis, controlling HSC quiescence, and maintaining HSC homeostasis, as well as in leukemogenesis (9, 10, 13–16). Numerous genetic studies have demonstrated that hyperactivation of mTOR by deletion of one of its negative regulators, including PTEN (9, 10), TSC1/TSC2 (11), PML (17), or ITPKB (18), can drive HSCs from quiescence into active cell cycling and cause subsequent HSC expansion and transformation. Deregulation of mTOR signaling occurs frequently in various cancers, including hematologic malignancies, and contributes to leukemia progression, chemoresistance, and unfavorable outcomes (19–23); therefore, therapeutic targeting of mTOR is a hotly pursued strategy in anticancer therapies. Various mTOR inhibitors have been investigated as single or combination agents in clinical trials (24). However, the first-generation allosteric mTOR inhibitors, such as rapamycin and rapalogs that are only effective toward mTORC1, have shown limited anticancer efficacy in numerous clinical settings due to incomplete blockade of mTORC1 activity, inability to suppress mTORC2, and induced resistance (25, 26). The second-generation mTOR kinase inhibitors, developed with the aim to block the activity of both mTORC1 and mTORC2, are also showing limited benefits in clinical trials, as tumor cells can develop resistance by acquiring mTOR genetic mutations or evasively bypassing mTOR to favor cancer cell proliferation (27, 28). Therefore, understanding the mechanisms leading to resistance

Significance

mTOR plays a critical role in regulating cell growth and is an important anticancer target. Numerous studies using mTOR inhibitors have shown that mTOR targeting suppresses gene expression and cell proliferation. However, mTOR-targeted cancer therapies have seen very limited success, and evasive resistance to mTOR-targeted drugs needs to be addressed. By examining *mTOR* gene-deleted mouse hematopoietic stem cells, which show a loss of quiescence and hyperproliferation, we uncovered the activation of the ERK/MNK/eIF4E/RNA polymerase II/c-Myc axis as an adaptive mechanism to *mTOR* loss that results in increased chromatin accessibility and activated global gene expression, allowing the cells to hyperproliferate. The work also implicates a potential strategy for overcoming evasive resistance in mTOR-targeted therapies for leukemia.

Author contributions: C.F. and Y.Z. designed research; C.F., C.Z., M.K., Z.T., X. Cai, A.K.D., C.L.H., and X. Chen performed research; F.G., G.H., M.A., W.T., and Q.R.L. contributed new reagents/analytic tools; C.F., F.Z., L.X., and Y.Z. analyzed data; and C.F. and Y.Z. wrote the paper.

The authors declare no competing interest.

This article is a PNAS Direct Submission.

Published under the PNAS license.

[1]To whom correspondence may be addressed. Email: yi.zheng@cchmc.org.

This article contains supporting information online at https://www.pnas.org/lookup/suppl/doi:10.1073/pnas.2020102118/-/DCSupplemental.

Published December 28, 2020.

Downloaded at Palestinian Territory, occupied on December 11, 2021

www.manaraa.com

to mTOR targeting is essential for the rational design of mTOR-targeted therapies.

To determine the function of mTOR in HSC regulation, we previously developed a conditional *Mx-Cre;mTOR*$^{flox/flox}$ mouse model to inducibly delete *mTOR* in the BM, and found that *mTOR* loss drastically reduced BM cellularity and caused a transient increase in the number of HSCs. Strikingly, *mTOR* deletion led to a loss of quiescence and increased proliferation of HSCs without affecting survival (29), contrary to conventional expectations based on mTOR inhibition (30, 31). Here, we define the adaptive mechanism of HSC and progenitor hyperproliferation that results in increased chromatin accessibility and activated global gene expression upon mTOR loss. We further implicate this mechanism in the development of evasive resistance in leukemia in the context of prolonged mTOR inhibition.

Results

***mTOR* Gene Deletion Causes Hyperproliferation and Loss of Quiescence in HSCs.** To examine the function of mTOR in HSC regulation, we used the conditional *Mx1-Cre*$^{+/-}$*;mTOR*$^{flox/flox}$ and *Mx1-Cre*$^{-/-}$*;mTOR*$^{flox/flox}$ mice to produce the *mTOR*$^{-/-}$ and *mTOR*$^{flox/flox}$ genotypes [hereafter termed mTOR KO and wild type (WT), respectively] by polyinosine-polycytidine (pIpC) inductions. A PCR analysis confirmed the complete deletion of the *mTOR* gene in BM cells from the mTOR KO mice (*SI Appendix*, Fig. S1*A*). Western blotting further confirmed the ablation of mTOR protein expression, and the concomitantly reduced mTOR downstream effector activities, including phospho-ribosomal protein S6 (S6; S240/244), phospho-*eIF4E-binding protein* 1 (4E-BP1; T37/46), and phospho-AKT (S473), while phospho-AKT (T308) was elevated in a compensatory manner (Fig. 1 *A* and *B*). The mTOR KO mice died around 2 wk post pIpC injection due to pancytopenia as described previously (29) (*SI Appendix*, Fig. S1*B*). Transplantation of the BM cells from the mTOR KO mice resulted in recipient deaths within 2 wk (*SI Appendix*, Fig. S1*C*), confirming that *mTOR* loss impairs hematopoietic stem and progenitor cell (HSPC) engraftment.

At the stem/progenitor cell level, the mTOR KO BM cells formed few colonies when cultured in methylcellulose medium, suggesting that mTOR deficiency impairs the colony-forming ability of HSPCs (*SI Appendix*, Fig. S1 *D* and *E*). In vivo, *mTOR* deletion caused a drastic expansion of LK (Lin$^-$c-Kit$^+$) and LSK (Lin$^-$Sca-1$^+$c-Kit$^+$) cell populations, which account for 2.7% and 0.9% of the mTOR KO BM, compared with 0.7% and 0.1% of the WT BM, respectively (Fig. 1*C*). Moreover, the absolute number of mTOR KO HSCs (Lin$^-$Sca-1$^+$c-Kit$^+$CD135$^-$) was about fourfold higher than that of WT controls (Fig. 1 *D* and *E*). Cell cycle analysis found that, upon *mTOR* deletion, the quiescent (G0) subsets of HSCs were significantly reduced, whereas the active cycling G1 and S/G2/M cells were increased (Fig. 1*F*). No significant difference in apoptosis was detected in the mTOR KO HSCs compared with WT controls (*SI Appendix*, Fig. S1 *F* and *G*). The decrease in G0 cells and subsequent increase in G1/S/G2/M cells indicate a shift in the HSCs from quiescence to proliferation.

mTOR Gene Targeting Increases Global Chromatin Accessibility and Promotes Gene Activation in HSCs. To determine the mechanism by which mTOR KO HSCs become hyperproliferative, we assessed the impact of *mTOR* loss on chromatin accessibility of mTOR WT and KO HSCs by the assay for transposase-accessible chromatin using sequencing (ATAC-seq). Previous studies have established that mTOR inhibition by pharmacologic inhibitors suppresses chromatin accessibility and gene expression, ultimately inhibiting cell growth (30, 31). Our ATAC-seq analysis of the WT HSCs after 10 h treatment with 200 nM of the mTOR kinase inhibitor AZD2014 or 1 μM rapamycin confirmed the repressive effects of these mTOR inhibitors on chromatin accessibility of the HSCs, as the chromatin accessibility was markedly decreased in

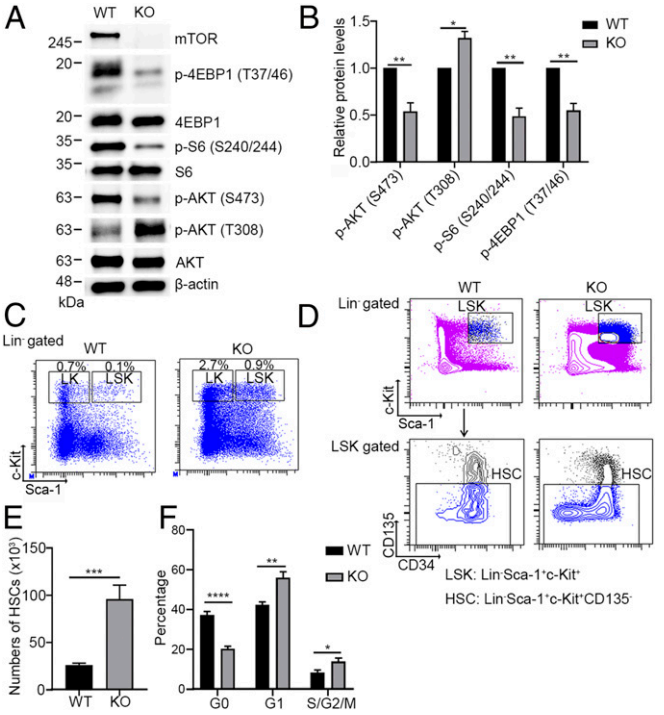

Fig. 1. mTOR KO HSCs lose quiescence and are hyperproliferative. (*A*) Representative immunoblotting for mTOR signaling components in LK (Lin$^-$c-Kit$^+$) cells from WT and mTOR KO mice. (*B*) Quantification of protein expression levels relative to β-actin, with the ratios in WT normalized to 1. Data represent mean ± SEM from three independent experiments. (*C*) Representative FACS profiles of the LK (Lin$^-$c-Kit$^+$) and LSK (Lin$^-$Sca-1$^+$c-Kit$^+$) cells from WT and mTOR KO mice. Numbers represent the average percentage in total BM cells for each fraction. (*D*) Representative FACS gating strategy to analyze HSCs (Lin$^-$Sca-1$^+$c-Kit$^+$CD135$^-$). Cell-surface makers to identify specific populations are indicated. (*E*) Absolute number of HSCs in total BM of WT and mTOR KO mice ($n = 5$ per genotype). (*F*) Cell cycle was analyzed by flow cytometry of Ki67 and 7-AAD staining. Proportions of mTOR WT and KO HSCs in each cell cycle phase are indicated ($n = 6$ per genotype). Data represent mean ± SEM (*$P < 0.05$, **$P < 0.01$, ***$P < 0.001$, ****$P < 0.0001$, two-tailed unpaired *t* test in *B*, *E*, and *F*). ns, not significant.

inhibitor-treated cells (Fig. 2 *A* and *B*). However, contrary to the effects by mTOR inhibitors, mTOR KO HSCs enhanced global chromatin accessibility, with remarkably increased signals compared with WT HSCs (Fig. 2 *C* and *D*). Consistent with the chromatin accessibility changes, chromatin immunoprecipitation sequencing (ChIP-seq) profiles of both H3K27Ac and H3K4me3, active chromatin marks correlating with active gene transcription, revealed globally activated patterns in mTOR KO HSCs. The signals for H3K27Ac and H3K4me3 at peaks nearing cell growth-related genes such as *c-Myc*, *Ccnd1*, *Dusp1*, *Fos*, *Jun*, and *Pim1* were markedly increased, suggestive of their transcriptional activation (Fig. 2*E–H*).

To examine the gene-expression changes associated with HSC hyperproliferation upon *mTOR* loss, we performed RNA sequencing (RNA-seq) of HSCs. We identified 1,589 differentially expressed genes (fold change ≥1.3, false discovery rate [FDR] <0.05), of which 720 genes and 869 genes were up-regulated and down-regulated, respectively, in mTOR KO HSCs compared with WT cells (Fig. 2*I*). Of note, well-known proliferation-associated genes such as *c-Myc*, *Dusp1*, *Fos*, *Jun*, and *Pim1* were significantly up-regulated in mTOR KO HSCs (Fig. 2*I*). Kyoto Encyclopedia of Genes and Genomes (KEGG) pathway and Gene Ontology (GO) functional enrichment analyses revealed that genes up-regulated in mTOR KO HSCs were enriched in ribosome, MAPK, Jak-Stat, translation, regulation of mitotic

Downloaded at Palestinian Territory, occupied on December 11, 2021
www.manaraa.com

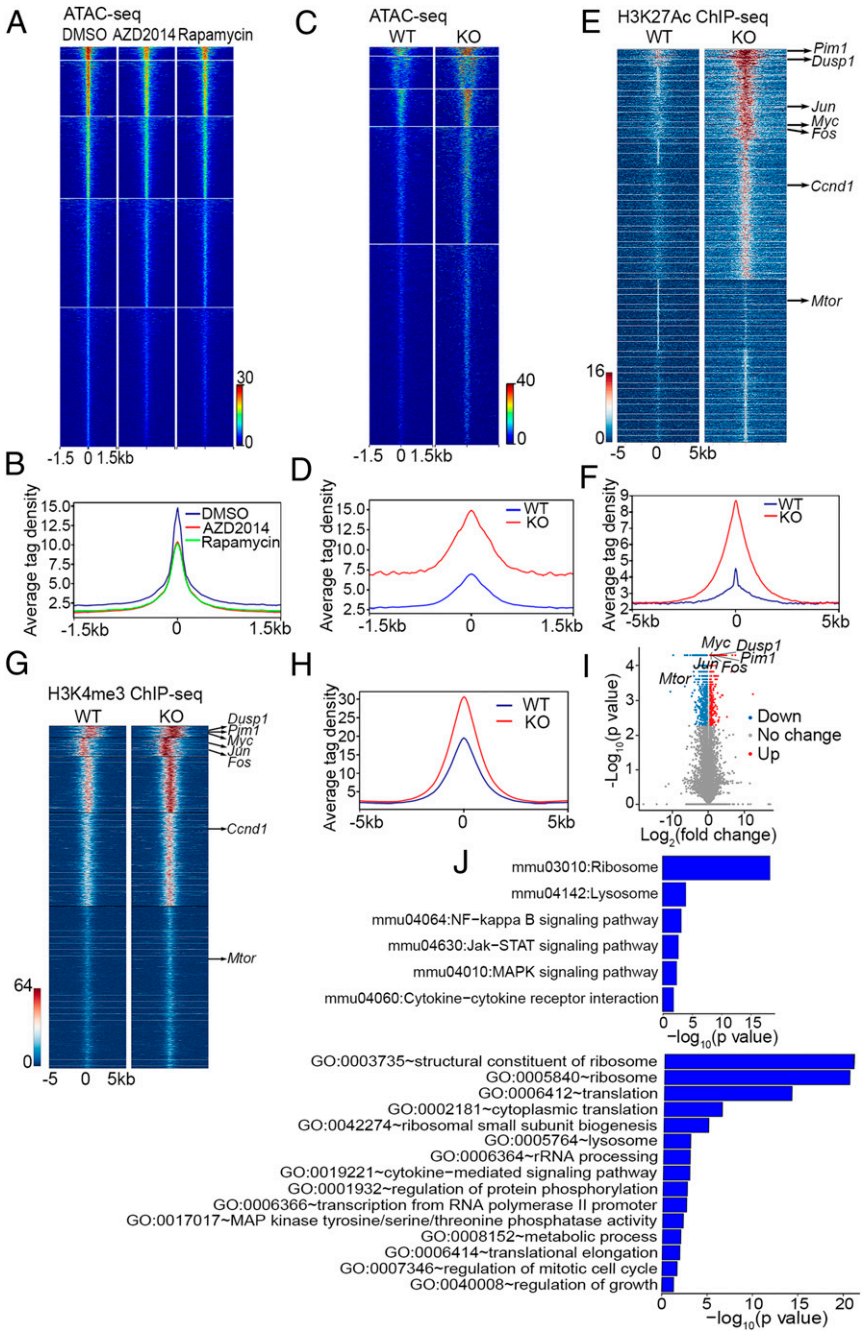

Fig. 2. *mTOR* gene targeting enhances global chromatin accessibility and promotes gene activation in HSCs. (*A* and *B*) HSCs isolated from 16 WT mice were treated with DMSO, 1 μM rapamycin, or 200 nM AZD2014, followed by ATAC-seq analysis. ATAC-seq density heat maps (*A*) and tag enrichment profiles (*B*) within ±1.5 kb around the peak center are shown. (*C* and *D*) HSCs from WT and mTOR KO mice ($n = 5$ mice for each genotype) were isolated and pooled by genotype. A total of 50,000 HSCs were used for ATAC-seq. ATAC-seq density heat maps (*C*) and tag enrichment profiles (*D*) within ±1.5 kb around the peak center in HSCs are shown. Data are representative of two independent biological repeats. (*E* and *F*) For each ChIP-seq experiment, HSCs from 28 WT and 11 mTOR KO mice were purified by FACS. The sorted cells were pooled by genotype, and half a million HSCs were used for ChIP-seq. ChIP-seq density heat maps (*E*) and tag enrichment profiles (*F*) for H3K27Ac within ±5 kb around the peak center in WT and mTOR KO HSCs. (*G* and *H*) ChIP-seq density heat maps (*G*) and tag enrichment profiles (*H*) for H3K4me3 within ±5 kb around the peak center in WT and mTOR KO HSCs. (*I*) HSCs from WT and mTOR KO mice ($n = 4$ mice per genotype) were used for RNA-seq, and volcano plot of differentially expressed transcripts is shown. Red and blue dots respectively represent genes significantly up-regulated and down-regulated in mTOR KO HSCs (FDR <0.05, fold change ≥1.3, $n = 4$ per genotype). (*J*) Overrepresented KEGG pathways and GO terms in the genes up-regulated in mTOR KO HSCs compared with WT controls.

cell cycle, and regulation of cell growth pathways (Fig. 2*J* and *SI Appendix*, Fig. S2 *A* and *B*). These enriched pathways are involved in promoting cell growth, consistent with the observed hyperproliferation phenotype of the mTOR KO HSCs. On the other hand, the down-regulated genes in the mTOR KO HSCs were enriched in cGMP-PKG, Rap1, cell junction, cell adhesion, and regulation of cell migration pathways, which may play roles in the homeostatic maintenance of HSCs by controlling their homing, mobilization, and retention within the BM niche (32) (*SI Appendix*, Fig. S2*C*). Gene Set Enrichment Analysis (GSEA)

Downloaded at Palestinian Territory, occupied on December 11, 2021

www.manaraa.com

also found up-regulation of genes related to ribosome biogenesis in mTOR KO HSCs (*SI Appendix*, Fig. S2 *D* and *E*).

Together, these genomic signatures suggest that mTOR gene targeting initiates an adaptive mechanism different from that invoked by short-term pharmacologic inhibitors, leading to a more accessible chromatin landscape with enhanced transcription activation and sustaining HSC proliferation.

mTOR Loss Causes c-Myc Elevation and the Activation of C-MYC Targets. c-Myc regulates the balance between self-renewal and differentiation of HSCs (33); elevated expression of c-Myc can confer transcriptional amplification, global changes in chromatin structure, elevated ribosome biogenesis, and cell growth advantages (34, 35). The observation in our RNA-seq data that the *c-Myc* transcriptional level was increased in the mTOR KO HSCs prompted the question as to whether it is associated with hyperproliferation of mTOR KO HSCs. qRT-PCR analysis yielded that *c-Myc*, as well as several other proliferation-associated genes found in the ChIP-seq and RNA-seq studies, were up-regulated in mTOR KO HSCs (Fig. 3*A*). Western blotting confirmed elevated C-MYC protein in *mTOR*-deleted HSCs (Fig. 3*B*). Increased signals for H3K27Ac and H3K4me3 occupancies were also observed at the *c-Myc* locus, suggesting *c-Myc* transcription activation (Fig. 3*C*). Moreover, GSEA analysis revealed that C-MYC target gene signature was significantly increased in *mTOR*-deficient HSCs (Fig. 3 *D* and *E*).

To investigate the effects of elevated C-MYC on its genome-wide occupancy and to identify target genes directly regulated by C-MYC in HSCs upon *mTOR* deletion, we isolated WT and mTOR KO HSCs and performed ChIP-seq with a C-MYC–specific antibody. In mTOR KO HSCs, elevated c-Myc levels led to broadly increased C-MYC binding to target loci (Fig. 3 *F* and *G*). To identify the direct C-MYC target genes with altered expression in mTOR KO HSCs, we intersected the C-MYC–bound genes with those genes differentially expressed between mTOR KO and WT HSCs and found about 649 C-MYC–regulated targets (Fig. 3*H*). These C-MYC targets were involved in various cell-proliferation processes, including ribosome, MAPK, translation, and regulation of cell cycle pathways (Fig. 3*I*). Thus, elevated c-Myc expression in mTOR KO HSCs leads to transcriptional activation of C-MYC targets associated with cell hyperproliferation.

c-Myc Is Elevated in a Compensatory Manner to Enhance Chromatin Accessibility and Drive Proliferation of the mTOR$^{-/-}$ HSCs. With c-Myc expression increasing about twofold in mTOR KO HSCs, we hypothesized that the hyperproliferation and cell cycle phenotypes are due to the elevated c-Myc. To test this hypothesis, we used combined conditional gene targeting and pharmacologic intervention approaches. First, we generated *Mx1-Cre*$^{+/-}$;*mTOR*$^{flox/flox}$;*c-Myc*$^{+/flox}$ mice (termed mTOR KO;*Myc*$^{+/-}$ mice hereafter), in which two *mTOR* alleles and one *c-Myc* allele were ablated after pIpC induction (33, 36). A single *c-Myc* allele ablation in mTOR KO mice led to a drastic reduction in the absolute number of HSCs to a level comparable to that of WT mice (Fig. 4*A*). Cell-cycle analysis showed that the loss of one *c-Myc* allele resulted in a significant increase in G0 and a decrease in G1 phase, indicating that c-Myc reduction could rescue the cell-cycle phenotype of mTOR KO HSCs (Fig. 4*B*). Loss of one *c-Myc* allele had no effect on HSC survival (*SI Appendix*, Fig. S3*A*). ATAC-seq analysis showed that one *c-Myc* allele deletion markedly reduced the chromatin accessibility and mostly rescued this mTOR KO effect (*SI Appendix*, Fig. S3*B*). In addition, mTOR KO;*Myc*$^{+/-}$ HSCs displayed corrected *Jun*/*Fos* gene expressions to the level of WT cells (*SI Appendix*, Fig. S3*C*). These observations suggest that the elevation of c-Myc drives the adaptive responses of global chromatin change and *Jun*/*Fos* up-regulation of the mTOR KO HSCs. On the other hand, the mTOR KO;*Myc*$^{+/-}$ mice retained the phenotype of reduced BM cellularity as in the mTOR KO mice, indicating that defects of mTOR KO progenitors and mature blood cell production cannot be rescued by one *c-Myc* allele deletion (Fig. 4*C*).

To complement the genetic evidence, we also treated the mTOR KO and WT HSCs with a bromodomain and extraterminal domain (BET) inhibitor, JQ1, which is capable of c-Myc inhibition (37), and examined the effects on cell proliferation and cell cycle distribution. We confirmed that both c-Myc transcript and protein levels were significantly reduced by JQ1 treatment of the mTOR KO HSCs (*SI Appendix*, Fig. S3 *D* and *E*). The addition of 500 nM or 1 μM JQ1 caused a significant decrease in the cell numbers of mTOR KO HSCs, whereas the cell growth-inhibitory effects on the WT HSCs were only marginal when JQ1 was at 1 μM (Fig. 4*D*). Another c-Myc inhibitor, 10058-F4, showed a similar suppressive effect (*SI Appendix*, Fig. S3*F*), suggesting that mTOR KO cells are sensitive to c-Myc inhibition. Consistently, JQ1 treatment of mTOR KO HSCs for 24 or 48 h led to a drastic accumulation of cells in G0 and a significant reduction in G1 and S/G2/M phases (Fig. 4*E*) without affecting cell cycle regulator p21 or cell apoptosis (*SI Appendix*, Fig. S3 *G* and *H*), indicating that pharmacologic inhibition of c-Myc suppresses the adaptive cell-cycle activation of mTOR KO HSCs.

mTOR Loss Induces Adaptive RNAP II Protein Elevation That Regulates c-Myc in HSCs. The above findings led us to consider the mechanism by which *c-Myc* expression is elevated during *mTOR* loss. Since several studies have shown that there is an interregulation between RNAP II and c-Myc for global transcription regulation (38–40), we next examined the RNAP II regulation of *c-Myc* transcriptional activity in the *mTOR*-deficient HSCs. We probed the protein levels of RNAP II, Ser2-phosphorylated RNAP II (Ser2P), and Ser5-phosphorylated RNAP II (Ser5P) in mTOR WT and KO LK cells, as well as in HSCs, and found a significant increase of expression of these proteins in the mTOR KO cells (Fig. 5 *A* and *B*). However, the transcript levels of RNAP II showed no significant increase in *mTOR*-deficient HSCs (*SI Appendix*, Fig. S4 *A* and *B*). The protein synthesis inhibitor cycloheximide (CHX) selectively decreased RNAP II protein expression in the mTOR KO cells but not in the WT cells (*SI Appendix*, Fig. S4*C*), further suggesting that RNAP II protein translation, but not transcriptional activation, is the underlying mechanism of the observed RNAP II protein increase in mTOR KO cells.

To determine the role of the elevated RNAP II, we next treated mTOR WT and KO HSCs with a CDK9 inhibitor, BAY 1143572, which has been reported to inhibit phosphorylation at the serine 2 site of the RNAP II C-terminal domain (41). BAY 1143572 was able to significantly reduce the cell numbers of mTOR KO HSCs in a dose-dependent manner, displaying ∼25% and 47% reduction at 200 nM and 400 nM, respectively, compared with DMSO control. In contrast, it had less of an effect on cell growth of *mTOR* WT HSCs and only caused a marginal reduction in cell numbers, suggesting that the *mTOR*-deficient HSCs are more sensitive to RNAP II inhibition (Fig. 5*C*). Moreover, BAY 1143572 treatment resulted in a significant increase of mTOR KO HSCs in the G0 phase and a decrease in the G1 phase (Fig. 5*D*) without affecting p21 protein expression or cell survival (*SI Appendix*, Fig. S4 *D* and *E*), suggesting that the cell-cycle phenotype of mTOR deficiency is related to the elevated RNAP II activity.

In parallel, we observed in mTOR KO HSCs that C-MYC expression level was significantly reduced by the BAY 1143572 treatment (Fig. 5*E*), whereas the elevated RNAP II protein level showed no significant change upon the loss of one *c-Myc* allele (Fig. 5*F*). ChIP-qPCR assay of RNAP II revealed that RNAP II occupancy was dramatically increased throughout the promoter and gene body regions of *c-Myc* in mTOR KO HSCs (Fig. 5*G*). These results suggest that RNAP II regulates *c-Myc* transcription, thereby resulting in an elevation of c-Myc in mTOR KO

Downloaded at Palestinian Territory, occupied on December 11, 2021

www.manaraa.com

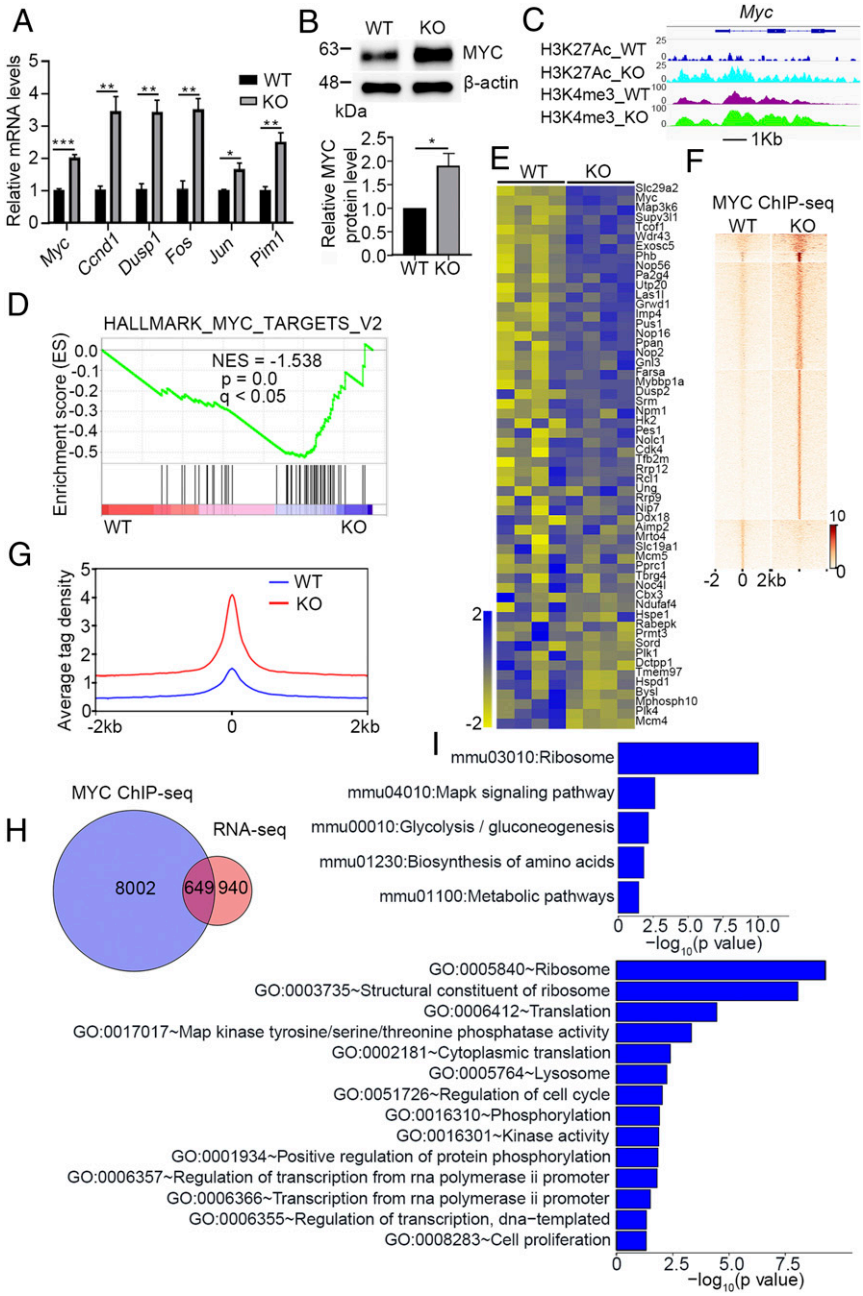

Fig. 3. *mTOR* loss causes c-Myc elevation and activation of C-MYC targets. (*A*) qRT-PCR analysis of transcript levels of indicated genes in WT and mTOR KO HSCs. Data represent mean ± SEM ($n = 3$; $^*P < 0.05$, $^{**}P < 0.01$, $^{***}P < 0.001$, two-tailed unpaired *t* test). (*B*, *Top*) Representative immunoblotting for C-MYC in WT and mTOR KO HSCs. (*B*, *Bottom*) Quantification of C-MYC expression relative to β-actin, with the ratio in WT normalized to 1. Data represent mean ± SEM from three independent experiments ($^*P < 0.05$, two-tailed unpaired *t* test). (*C*) ChIP-seq binding profiles for H3K27Ac and H3K4me3 at the *c-Myc* locus in WT and mTOR KO HSCs. (*D*) GSEA enrichment plot shows C-MYC target genes are up-regulated in mTOR KO HSCs ($n = 4$ per genotype). NES, normalized enrichment score. (*E*) Heat map of C-MYC target genes from GSEA enrichment analysis (in *D*) in WT and mTOR KO HSCs. (*F*) Heat map for C-MYC ChIP-seq peaks in WT and mTOR KO HSCs within ±2 kb around the peak center. (*G*) C-MYC ChIP-seq tag enrichment profile around the peak center. (*H*) Venn diagram shows the overlap between C-MYC–bound genes and differentially expressed genes in WT and mTOR KO HSCs in RNA-seq. The overlapping genes are direct C-MYC target genes. (*I*) Enrichment of KEGG pathways and GO terms overrepresented in C-MYC target genes.

HSCs. Interestingly, protein expression, but not RNA expression, of related RNA polymerase I (RNAP I) and polymerase III (RNAP III) was also found to be elevated in mTOR KO HSCs (*SI Appendix*, Fig. S4 *F–H*). The housekeeping histone proteins, H1, H2A, H2B, H3, and H4, however, remained unchanged (*SI Appendix*, Fig. S4*H*), indicating that *mTOR* loss causes a selective increase in protein expression of RNAP I, RNAP II, and RNAP III.

Adaptive ERK–MNK–eIF4E Activation in mTOR$^{-/-}$ HSCs Causes RNAP II Protein Elevation. Protein translational control plays a pivotal role in the regulation of gene expression and protein abundance in the adaptive response to stimuli (42). In mTOR KO HSCs, ribosome, translation, and MAPK pathways were up-regulated (Fig. 2*J*); we thus focused on the MAPK-interacting protein kinase (MNK), which can be activated by extracellular signal-regulated kinase (ERK) or p38 MAPK and may enhance translation

Downloaded at Palestinian Territory, occupied on December 11, 2021

www.manaraa.com

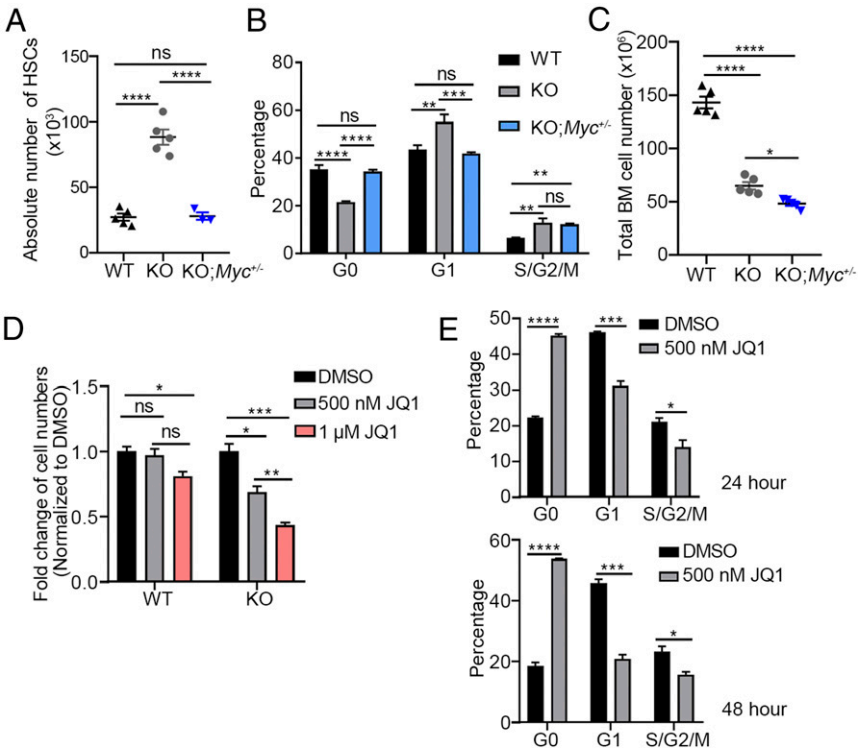

Fig. 4. The hyperproliferation phenotype of *mTOR*-deficient HSCs is due to compensatory c-Myc elevation. (*A*) Absolute number of HSCs in the BM of WT ($n = 5$), mTOR KO ($n = 5$), and mTOR KO;$Myc^{+/-}$ ($n = 3$) mice 5 d after the last pIpC injection. (*B*) Cell cycle was analyzed by flow cytometry of Ki67 and 7-AAD staining. The HSC proportions in indicated phases of cell cycle from WT ($n = 4$), mTOR KO ($n = 5$), and mTOR KO;$Myc^{+/-}$ ($n = 8$) mice are shown. (*C*) Total BM cellularity in WT, mTOR KO, and mTOR KO;$Myc^{+/-}$ mice ($n = 5$ per genotype). (*D*) Quantification of cell numbers for WT and mTOR KO HSCs treated with DMSO or JQ1 for 72 h. (*E*) mTOR KO HSCs were treated with DMSO or JQ1 for indicated times, and cell cycle was analyzed by flow cytometry of Ki67 and 7-AAD staining. The proportions in indicated phases of cell cycle are shown ($n = 3$). Data represent mean ± SEM (*$P < 0.05$, **$P < 0.01$, ***$P < 0.001$, ****$P < 0.0001$, one-way ANOVA in *A–D*, two-tailed unpaired *t* test in *E*). ns, not significant.

through phosphorylation of the eukaryotic translation initiation factor 4E (eIF4E) at Ser209 (43–45). Since the mTOR pathway and the MNK–eIF4E pathway interact in cancer cell proliferation and drug resistance (46, 47), we hypothesized that MNK–eIF4E activated by MAPK signaling may be responsible for the elevated protein level of RNAP II. To this end, we probed for the protein levels of phospho-MNK1 (T197/202), phospho-ERK (T202/Y204), and phospho-eIF4E (S209) by Western blotting in LSK cells and found that they were significantly up-regulated in the mTOR KO cells (Fig. 6 *A* and *B*). We also probed the phospho-p38 MAPK (T180/Y182) level but observed no change in mTOR KO cells (*SI Appendix*, Fig. S5*A*). Notably, the ERK inhibitor SCH772984 effectively inhibited MNK/eIF4E signaling, C-MYC, and RNAP II protein expression in mTOR KO cells (Fig. 6*C*). These results suggest that the elevated ERK activity, but not that of p38, causes the increased MNK/eIF4E signaling upon mTOR loss.

To evaluate the involvement of the MNK–eIF4E axis in the regulation of RNAP II protein expression, we treated mTOR KO LSKs with MNK inhibitor CGP 57380 (10 μM or 20 μM) and found that protein levels of phospho-MNK1, phospho-eIF4E, C-MYC, and RNAP II were markedly reduced, suggesting that a blockade of MNK activity can profoundly suppress phospho-eIF4E and RNAP II protein expression in the context of the adaptive responses in the mTOR KO cells (Fig. 6*D*). Moreover, the HSC population in G0 phase was significantly increased and cells in G1 phase were decreased (Fig. 6*E*), while the p21 level and cell survival remained unchanged upon CGP 57380 treatment of mTOR KO HSCs (*SI Appendix*, Fig. S5 *B* and *C*), indicating that MNK inhibition can revert the hyperproliferation phenotype of mTOR KO HSCs.

Interestingly, *mTOR*-deficient HSCs displayed an increased rate of protein synthesis compared to WT cells (Fig. 6*F*) despite the reduced canonical mTOR signaling in phosphorylated ribosomal protein S6 and 4E-BP1 (Fig. 1*A*). To examine whether the MNK/eIF4E axis is responsible for increased protein synthesis, we treated the mTOR WT and KO mice in vivo with an MNK inhibitor, eFT508, after pIpC induction, and observed that phospho-MNK1, phospho-eIF4E, C-MYC, and RNAP II were dramatically reduced in mTOR KO cells (*SI Appendix*, Fig. S5*D*). Parallel O-propargyl-puromycin (OPP) incorporation assay showed that the MNK inhibition reduced protein synthesis of the mTOR KO HSCs, but had no effect on global protein synthesis of the WT cells (Fig. 6*G*). These data suggest that the observed MNK/eIF4E effect on protein synthesis is due to the adaptive response of mTOR loss, in line with the previously reported role of MNK/eIF4E signaling (48–50), i.e., MNK/eIF4E axis does not increase global protein synthesis under WT conditions. In addition, the deletion of one *c-Myc* allele rescued the overall protein synthesis phenotype of mTOR KO cells without correcting the elevated RNAPII (Figs. 5*F* and 6*H*), suggesting that the increase in RNAP II-c-Myc mediates the global protein synthesis. Collectively, these results indicate that the adaptive response of the mTOR KO cells causes an ERK/MNK/eIF4E-mediated RNAP II up-regulation, which in turn results in a c-Myc–mediated global protein synthesis effect associated with an adaptive gene activation and cell proliferation.

mTOR Inhibitor-Resistant Leukemia Cells Mimic the mTOR$^{-/-}$ HSCs in the Adaptive MNK–RNAP II–c-Myc Response. While therapeutic targeting of mTOR in leukemia is a promising strategy, mTOR inhibitors were mostly ineffective in clinical trials, as tumor cells

Downloaded at Palestinian Territory, occupied on December 11, 2021
www.manaraa.com

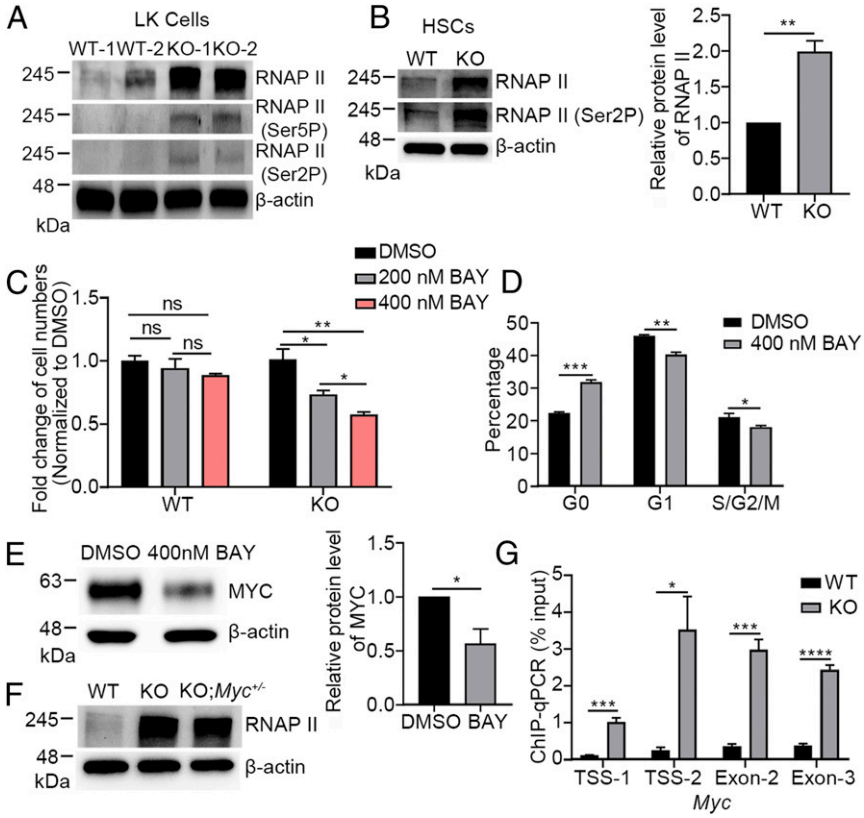

Fig. 5. Adaptive RNAP II protein elevation regulates c-Myc in mTOR KO HSCs. (*A*) Immunoblotting of RNAP II in LK cells from WT and mTOR KO mice. (*B*, *Left*) Representative immunoblotting for RNAP II in WT and mTOR KO HSCs. (*B*, *Right*) Quantification of RNAP II expression relative to β-actin, with the ratio in WT normalized to 1. Data represent mean ± SEM from three independent experiments. (*C*) Quantification of cell numbers for mTOR KO and WT HSCs treated with DMSO or BAY 1143572 for 72 h (normalized to DMSO for each group; $n = 3$). (*D*) The proportions in indicated phases of cell cycle in mTOR KO HSCs treated with DMSO or BAY 1143572 for 24 h ($n = 3$). (*E*) Representative immunoblotting (*Left*) and quantification (*Right*) of C-MYC in mTOR KO HSCs treated with DMSO or BAY 1143572 for 24 h. Data represent mean ± SEM from three independent experiments. (*F*) Immunoblotting of RNAP II in HSCs from WT, mTOR KO, and mTOR KO;*Myc*$^{+/-}$ mice. (*G*) ChIP-qPCR analysis of RNAP II at *c-Myc* locus in WT and mTOR KO HSCs ($n = 4$). Data represent mean ± SEM (*$P <$ 0.05, **$P < 0.01$, ***$P < 0.001$, ****$P < 0.0001$, two-tailed unpaired *t* test in *B*, *D*, *E*, and *G*; one-way ANOVA in *C*). ns, not significant.

tend to develop resistance by evading the mTOR-controlled cell growth machinery. Our findings in the mTOR KO HSCs prompted us to ask if leukemia cells can utilize a similar adaptive mechanism to elicit resistance to prolonged mTOR inhibition.

We employed BaF3 cells with constitutive BCR-ABL expression (BaF3-BA) (51) to screen for mTOR inhibitor-resistant variants. Exposure of the BaF3-BA cells to 1 μM AZD2014, a second-generation mTOR kinase inhibitor, resulted in multiple mTOR inhibitor-resistant leukemia clones (such as S11, S17, and S19) with significantly reduced phospho-4E-BP1 (T37/46; Fig. 7 *A* and *B*). Western blotting confirmed the constitutively reduced canonical mTOR signaling activities through phospho-S6 (S240/244) and a compensating elevated phospho-AKT (T308; Fig. 7*C*), mimicking that seen in the mTOR KO HSCs. The resistant leukemia cells also mimicked the mTOR KO HSCs in possessing elevated RNAP II and C-MYC compared with those in BaF3-BA parental cells (Fig. 7*D*). The reduced mTOR signaling caused a compensatory elevation of phospho-MNK1 (T197/202), phospho-ERK (T202/Y204), and phospho-eIF4E (S209) as seen by Western blotting (Fig. 7*E*). As we found in the mTOR KO HSCs, such adaptive responses of phospho-eIF4E, C-MYC, and RNAP II in AZD2014-resistant single-clone S11 cells were due to the increased MAPK and the MNK activity, since their levels could be suppressed after treatment with MNK inhibitor CGP 57380 (Fig. 7*F*).

Last, BET, CDK9, or MNK inhibitor (JQ1, BAY 1143572, or CGP 57380) treatment of the AZD2014-resistant leukemia cells selectively reduced the cell proliferation (Fig. 7 *G*–*I*), suggesting that the mTOR inhibitor-resistant leukemia cells are more sensitive to c-Myc, RNAP II, and MNK inhibition. Together, these results suggest that mTOR inhibitor-resistant leukemia cells can adopt a similar adaptive proliferative mechanism to that seen in mTOR KO HSCs.

Discussion

mTOR is an essential regulator of hematopoiesis and HSC maintenance (13, 15, 16). Multiple studies have established that hyperactivation of mTOR through ablation of negative regulators (9–11, 17) or by overexpression of mTOR activators (52) causes increased cell cycle rate, transient increase of HSC numbers, and exhaustion of HSCs. However, contrary to the anticipated decrease in cell growth due to mTOR inhibition, in the *mTOR* loss-of-function studies using *Mx1-Cre*$^{+/-}$;*mTOR*$^{flox/flox}$ mice, we found that deletion of *mTOR* in mouse BM resulted in a loss of quiescence and hyperproliferation of the HSCs (Fig. 1) (29). The underlying mechanisms are likely related to compensatory adaptation, which provides a unique opportunity to better understand the role of mTOR in hematopoiesis and in the development of adaptive resistance to mTOR-targeted therapies.

Our ATAC-seq analyses revealed that *mTOR* WT HSCs displayed decreased chromatin accessibility after treatment with mTOR inhibitors (Fig. 2), consistent with previously reported effects of mTOR inhibition (30, 31). However, mTOR KO HSCs showed the opposite effects, with increased chromatin accessibility

Downloaded at Palestinian Territory, occupied on December 11, 2021

www.manaraa.com

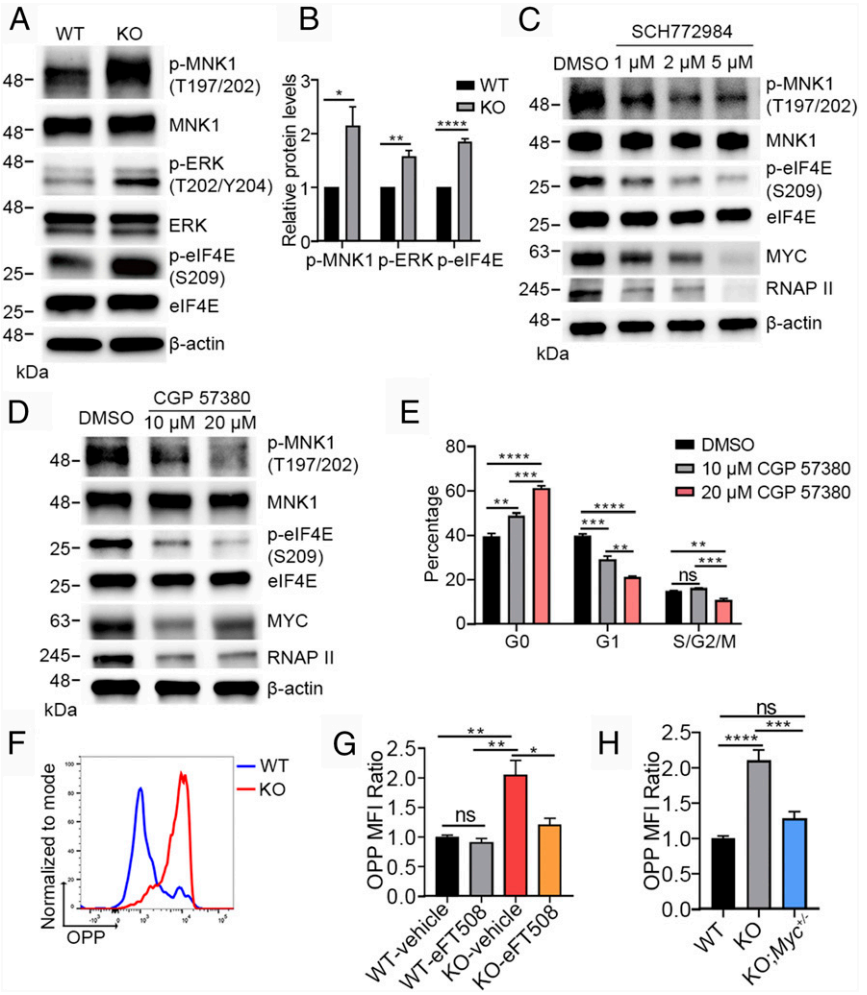

Fig. 6. Elevated ERK–MNK–eIF4E axis provides a compensatory pathway for maintaining protein synthesis and proliferation in mTOR KO cells. (*A*) Representative immunoblotting for phospho-MNK1 (T197/202), phospho-ERK (T202/Y204), and phospho-eIF4E (S209) in WT and mTOR KO LSK cells. (*B*) Quantification of protein expression levels relative to β-actin, with the ratios in WT normalized to 1. Data represent mean ± SEM from at least three independent experiments. (*C*) Immunoblotting for phospho-MNK1 (T197/202), phospho-eIF4E (S209), C-MYC, and RNAP II in mTOR KO LSK cells treated with the ERK inhibitor SCH772984 for 24 h. (*D*) Immunoblotting for phospho-MNK1 (T197/202), phospho-eIF4E (S209), C-MYC, and RNAP II in mTOR KO LSK cells treated with CGP 57380 for 24 h. (*E*) mTOR KO HSCs were treated with DMSO or CGP 57380 for 24 h, and cell cycle was analyzed by flow cytometry using Ki67 and 7-AAD staining. The proportions in indicated phases of the cell cycle are shown. (*F*) Representative histogram shows OPP incorporation into HSCs isolated from WT (blue) and mTOR KO (red) mice. (*G*) WT and mTOR KO mice ($n = 3$ mice per genotype) were treated daily for 5 d post pIpC injection with vehicle or 10 mg/kg eFT508 by oral gavage. Then the relative protein synthesis rates of HSCs were quantified by flow cytometry of OPP, normalized to the geometric mean fluorescence intensity (MFI) of OPP in WT vehicle condition. (*H*) The relative protein synthesis rates in WT, mTOR KO, and mTOR KO;*Myc*$^{+/-}$ HSCs were quantified by flow cytometry of OPP, normalized to MFI of OPP in WT group ($n = 3$). Data represent mean ± SEM (*$P < 0.05$, **$P < 0.01$, ***$P < 0.001$, ****$P < 0.0001$, two-tailed unpaired *t* test in *B*; one-way ANOVA in *E*, *G*, and *H*). ns, not significant.

after genetic deletion (Fig. 2). The discrepancy between genetic and pharmacological approaches to inhibit mTOR activity is likely due to differences in the duration and extent of the inhibition vs. gene targeting. ChIP-seq analyses in mTOR KO HSCs found globally increased signals for both H3K27Ac and H3K4me3 marks, indicative of active enhancers and promoters of active chromatins (Fig. 2) (53–55). These genome-wide studies indicate that *mTOR* gene loss leads to more accessible chromatins in HSCs, which allows consequential activation of genes.

Our mRNA transcriptome profiling saw a significant up-regulation of proliferation-associated genes and an enrichment of related pathways, including *c-Myc*, *Fos*, *Jun*, MAPK, ribosome, and Jak-Stat pathways (Fig. 2). The C-MYC targets were enriched in proliferation-related pathways such as ribosome and MAPK signaling (Fig. 3). Genetic rescue experiments in *mTOR*-deficient HSCs by ablation of one *c-Myc* allele in mTOR KO mice or by pharmacologic inhibition with BET inhibitor JQ1 were able to revert the HSC cell number and cell cycle phenotype (Fig. 4). Moreover, ATAC-seq analyses showed that the loss of one *c-Myc* allele in mTOR KO HSCs reduced the chromatin accessibility effect (*SI Appendix*, Fig. S3). Thus, the compensatory elevation of c-Myc is essential in the adaptive responses of the mTOR KO cells, including increased gene activation and chromatin accessibility.

The protein level of RNAP II in mTOR KO HSCs was elevated, and the RNAP II-suppressing CDK9 inhibitor BAY 1143572 reduced the cell numbers and restored the cell-cycle phenotype of mTOR KO HSCs (Fig. 5), indicating that RNAP II contributes to the hyperproliferation of *mTOR*-deficient HSCs. ChIP-qPCR assay of RNAP II at the *c-Myc* locus found that RNAP II occupancy was significantly increased throughout the gene body of *c-Myc* in mTOR KO HSCs (Fig. 5), suggesting that RNAP II regulates *c-Myc* transcription and causes elevated

Downloaded at Palestinian Territory, occupied on December 11, 2021
www.manaraa.com

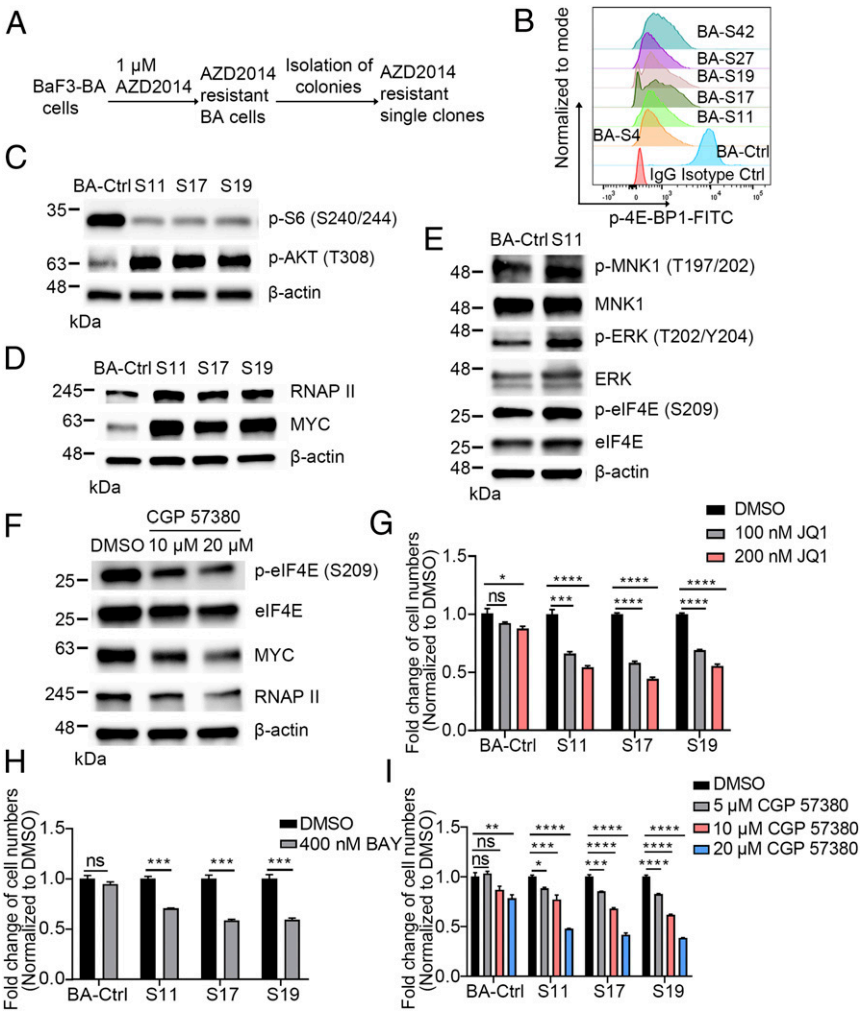

Fig. 7. mTOR inhibitor-resistant leukemia cells mimic mTOR KO HSCs in utilizing the MNK–RNAP II–c-Myc cascade for proliferation. (*A*) Schematic for in vitro screen of mTOR inhibitor (1 μM AZD2014)-resistant BaF3-BA single clones. (*B*) Intracellular staining of phospho-4E-BP1 (T37/46) in AZD2014-resistant BaF3-BA single clones and parental control measured by flow cytometry. (*C* and *D*) Immunoblotting for phospho-S6 (S240/244) and phospho-AKT (T308; *C*) and for RNAP II and C-MYC (*D*) in indicated AZD2014-resistant BaF3-BA single clones and parental control. (*E*) Immunoblotting for phospho-MNK (T197/202), phospho-ERK (T202/Y204), and phospho-eIF4E (S209) in AZD2014-resistant BaF3-BA single clone S11 and parental control cells. (*F*) Immunoblotting for phospho-eIF4E (S209), C-MYC, and RNAP II in AZD2014-resistant BaF3-BA single-clone S11 treated with CGP 57380 for 24 h. (*G, H,* and *I*) Quantification of cell numbers for indicated AZD2014-resistant BaF3-BA single clones and parental control treated with DMSO or JQ1 (*G*), BAY 1143572 (*H*), or CGP 57380 (*I*) for 72 h. Data represent mean ± SEM ($n = 3$; *$P < 0.05$, **$P < 0.01$, ***$P < 0.001$, ****$P < 0.0001$; *G* and *I*, one-way ANOVA; *H*, two-tailed unpaired *t* test). ns, not significant.

c-Myc expression, thereby leading to HSC hyperproliferation. Interestingly, despite the RNAP II elevation at the protein level, the transcriptional level of RNAP II was not significantly increased in *mTOR*-deficient HSCs (*SI Appendix*, Fig. S4). In addition, the protein synthesis inhibitor CHX selectively suppressed RNAP II protein expression in the mTOR KO cells but not in the WT cells (*SI Appendix*, Fig. S4), suggesting that the elevated RNAP II protein in mTOR KO cells is due to RNAP II protein translation, not transcriptional activation. Indeed, the posttranscriptional increase of RNAP II appears essential for the adaptive response of *mTOR*-deficient HSCs. Previously, activation of mTORC1 has been shown to promote protein synthesis while also increasing the capacity of proteasome-mediated protein degradation through nuclear factor erythroid 2-related factor 1 (Nrf1; also known as Nfe2l1), whose transcription is induced by sterol regulatory element binding transcription factor 1 (Srebf1; also known as Srebp1) (56). In our case, the mRNA levels of *Srebf1* and *Nfe2l1* in mTOR KO HSCs did not change compared with WT controls, suggesting that the effect is through an *Srebf1*- and *Nfe2l1*-independent mechanism.

In eukaryotes, activated mTORC1 phosphorylates downstream targets S6K1 and 4E-BP1 to allow cap-dependent translation (57). Despite decreased canonical mTOR signaling, mTOR KO HSCs were able to compensate with an increased protein synthesis rate, bypassing the mTOR/4E-BP1/eIF4E axis to promote translation and induce RNAP II protein elevation (Figs. 1 and 6). The ribosome and MAPK pathways were up-regulated in mTOR KO HSCs, and elevated MAPK/MNK can promote translation activity through phosphorylation of eIF4E at Ser209 (43–45). Indeed, the compensatory response of the ERK/MNK/eIF4E pathway was adaptively activated during *mTOR* loss (Fig. 6). Moreover, protein levels of RNAP II and C-MYC in mTOR KO LSKs, and consequently global protein synthesis as well as the cell cycle rate in KO HSCs, were reduced by an MNK inhibitor (Fig. 6). Thus, a rewired ERK–MNK–eIF4E axis is involved in the adaptive response to *mTOR* loss in protein translation, leading to hyperproliferation of mTOR KO HSCs. We also found that one *c-Myc* allele deletion

Downloaded at Palestinian Territory, occupied on December 11, 2021

www.manaraa.com

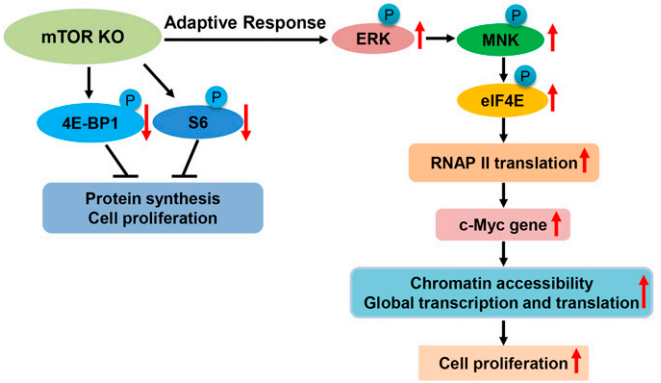

Fig. 8. A model of the adaptive responses to mTOR loss in HSPCs. Loss of *mTOR* causes a compensatory elevation of ERK activity, leading to increased MNK/eIF4E signaling and consequent RNAP II protein translation. The increased RNAP II protein level causes *c-Myc* gene up-regulation, which is responsible for the global transcription and translation up-regulation and associated cell hyperproliferation.

can reduce the protein synthesis in mTOR KO HSCs (Fig. 6), suggesting that elevated c-Myc drives the increased protein synthesis upon mTOR loss. Taken together, we propose a mechanism of the adaptive response to mTOR loss in which mTOR loss causes a compensatory elevation of ERK/MNK/eIF4E signaling and RNAP II protein translation, consequently increasing RNAP II protein and c-Myc expression, which is responsible for the global transcription and translation up-regulation (Fig. 8).

mTOR-targeted therapies are currently in clinical trials to combat the increased mTOR signaling found in many human cancers, including leukemia (19–24, 58, 59). However, the strategy has yet to show major benefits, in part due to widespread resistance to both the first- and second-generation mTOR inhibitors (25–28). Other than innate resistance derived from mutations in *mTOR* itself, evasive resistance from adaptive compensations may also play a role. To this end, activation of compensatory signaling such as MAPK or PI3K/Akt has been implicated in mTOR targeting resistance (60).

We found that the adaptive response observed in the $mTOR^{-/-}$ HSCs appears to be similarly adopted in mTOR inhibitor-resistant leukemia cells. A compensatory MNK–RNAP II–c-Myc cascade can contribute to maintaining leukemia cell proliferation by evading mTOR-controlled protein synthesis and normal cell growth machineries after long-term exposure to mTOR inhibitors (Fig. 7). These insights provided from the mTOR KO HSC studies are valuable for developing alternative strategies to overcome such resistance. In the case of leukemia cells that have acquired adaptive resistance, the use of BET inhibitors to suppress c-Myc, a CDK9 inhibitor which controls RNAP II activity, or an MNK inhibitor which suppresses RNAP II translation, can have potential benefits in suppressing the evasive mTOR drug resistance (Fig. 7).

Our work adds significantly to previous studies that identified MEK/ERK, GSK3β/β-catenin, and PI3K/Akt pathways as mechanisms of mTOR targeting resistance (60). It further rationalizes that a combinatory treatment targeting multiple pathways involved in the adaptive responses should be taken into consideration when developing therapies.

Materials and Methods

Mice. Mouse strains of $mTOR^{flox/flox}$ and $c\text{-}Myc^{flox/flox}$ were previously described (61, 62). All animal experiments were approved by the institutional animal care and use committee at Cincinnati Children's Hospital Medical Center.

HSC Isolation. LK ($Lin^-c\text{-}Kit^+$), LSK ($Lin^-Sca\text{-}1^+c\text{-}Kit^+$), and HSC ($Lin^-Sca\text{-}1^+c\text{-}Kit^+CD135^-$) subpopulations were identified with surface markers. Flow cytometry cell sorting was performed on a FACSAria II device (BD Biosciences).

OPP Assay. An OPP-labeling assay was performed to measure in vivo global protein synthesis rates of HSCs as previously reported (63).

Statistics. All data are presented as mean ± SEM unless otherwise specified. Statistical significance was determined using two-tailed unpaired *t* test or one-way ANOVA followed by Tukey/Dunnett's tests.

Detailed materials and methods, including mice, BM transplantation and survival analysis, colony formation assay, drugs, flow cytometry analysis and HSC isolation, apoptosis assay, cell cycle analysis, OPP assay, phospho-flow analysis, cell culture, generation of mTOR inhibitor-resistant leukemia single clones, cell growth assay, Western blot assays, RNA isolation and quantitative real-time PCR, RNA-seq and data analysis, ChIP-seq, ATAC-seq, ChIP-qPCR assay, and statistics are available in *SI Appendix, SI Materials and Methods*.

Data Availability. All of the RNA-seq, ChIP-seq, and ATAC-seq data reported in this paper have been deposited in the National Center for Biotechnology Information Gene Expression Omnibus database under accession numbers GSE134316 and GSE134317.

ACKNOWLEDGMENTS. We thank James Johnson for technical assistance. We are thankful to the Research Flow Cytometry Core and the Comprehensive Mouse and Cancer Core for technical support. The work was partially supported by Cancer Free Kids (308269).

1. C. J. Eaves, Hematopoietic stem cells: Concepts, definitions, and the new reality. *Blood* **125**, 2605–2613 (2015).
2. S. H. Orkin, L. I. Zon, Hematopoiesis: An evolving paradigm for stem cell biology. *Cell* **132**, 631–644 (2008).
3. D. T. Scadden, The stem-cell niche as an entity of action. *Nature* **441**, 1075–1079 (2006).
4. A. Trumpp, M. Essers, A. Wilson, Awakening dormant haematopoietic stem cells. *Nat. Rev. Immunol.* **10**, 201–209 (2010).
5. A. Wilson *et al.*, Hematopoietic stem cells reversibly switch from dormancy to self-renewal during homeostasis and repair. *Cell* **135**, 1118–1129 (2008).
6. I. Beerman, T. C. Luis, S. Singbrant, C. Lo Celso, S. Méndez-Ferrer, The evolving view of the hematopoietic stem cell niche. *Exp. Hematol.* **50**, 22–26 (2017).
7. L. M. Calvi, D. C. Link, The hematopoietic stem cell niche in homeostasis and disease. *Blood* **126**, 2443–2451 (2015).
8. B. Krock, N. Skuli, M. C. Simon, The tumor suppressor LKB1 emerges as a critical factor in hematopoietic stem cell biology. *Cell Metab.* **13**, 8–10 (2011).
9. O. H. Yilmaz *et al.*, Pten dependence distinguishes haematopoietic stem cells from leukaemia-initiating cells. *Nature* **441**, 475–482 (2006).
10. J. Zhang *et al.*, PTEN maintains haematopoietic stem cells and acts in lineage choice and leukaemia prevention. *Nature* **441**, 518–522 (2006).
11. C. Chen *et al.*, TSC-mTOR maintains quiescence and function of hematopoietic stem cells by repressing mitochondrial biogenesis and reactive oxygen species. *J. Exp. Med.* **205**, 2397–2408 (2008).
12. R. A. Saxton, D. M. Sabatini, mTOR signaling in growth, metabolism, and disease. *Cell* **168**, 960–976 (2017).
13. T. Hoshii, S. Matsuda, A. Hirao, Pleiotropic roles of mTOR complexes in haemato-lymphopoiesis and leukemogenesis. *J. Biochem.* **156**, 73–83 (2014).
14. D. Meng, A. R. Frank, J. L. Jewell, mTOR signaling in stem and progenitor cells. *Development* **145**, dev152595 (2018).
15. D. Kalaitzidis *et al.*, mTOR complex 1 plays critical roles in hematopoiesis and Pten-loss-evoked leukemogenesis. *Cell Stem Cell* **11**, 429–439 (2012).
16. B. Gan, R. A. DePinho, mTORC1 signaling governs hematopoietic stem cell quiescence. *Cell Cycle* **8**, 1003–1006 (2009).
17. K. Ito *et al.*, PML targeting eradicates quiescent leukaemia-initiating cells. *Nature* **453**, 1072–1078 (2008).
18. S. Siegemund *et al.*, IP3 3-kinase B controls hematopoietic stem cell homeostasis and prevents lethal hematopoietic failure in mice. *Blood* **125**, 2786–2797 (2015).
19. A. Kentsis, A. T. Look, Distinct and dynamic requirements for mTOR signaling in hematopoiesis and leukemogenesis. *Cell Stem Cell* **11**, 281–282 (2012).
20. J. Ghosh, R. Kapur, Role of mTORC1-S6K1 signaling pathway in regulation of hematopoietic stem cell and acute myeloid leukemia. *Exp. Hematol.* **50**, 13–21 (2017).
21. Y. Gao *et al.*, Rheb1 promotes tumor progression through mTORC1 in MLL-AF9-initiated murine acute myeloid leukemia. *J. Hematol. Oncol.* **9**, 36 (2016).
22. O. Lindblad *et al.*, Aberrant activation of the PI3K/mTOR pathway promotes resistance to sorafenib in AML. *Oncogene* **35**, 5119–5131 (2016).
23. A. Khanna *et al.*, High mTOR expression independently prognosticates poor clinical outcome to induction chemotherapy in acute lymphoblastic leukemia. *Clin. Exp. Med.* **18**, 221–227 (2018).
24. T. Calimeri, A. J. M. Ferreri, m-TOR inhibitors and their potential role in haematological malignancies. *Br. J. Haematol.* **177**, 684–702 (2017).
25. J. Heitman, N. R. Movva, M. N. Hall, Targets for cell cycle arrest by the immunosuppressant rapamycin in yeast. *Science* **253**, 905–909 (1991).
26. J. Kunz *et al.*, Target of rapamycin in yeast, TOR2, is an essential phosphatidylinositol kinase homolog required for G1 progression. *Cell* **73**, 585–596 (1993).

Downloaded at Palestinian Territory, occupied on December 11, 2021
www.manaraa.com

27. C. L. Cope *et al*., Adaptation to mTOR kinase inhibitors by amplification of eIF4E to maintain cap-dependent translation. *J. Cell Sci.* **127**, 788–800 (2014).
28. S. Mallya *et al*., Resistance to mTOR kinase inhibitors in lymphoma cells lacking 4EBP1. *PLoS One* **9**, e88865 (2014).
29. F. Guo *et al*., Mouse gene targeting reveals an essential role of mTOR in hematopoietic stem cell engraftment and hematopoiesis. *Haematologica* **98**, 1353–1358 (2013).
30. J. R. Rohde, M. E. Cardenas, The tor pathway regulates gene expression by linking nutrient sensing to histone acetylation. *Mol. Cell. Biol.* **23**, 629–635 (2003).
31. P. Sen, P. P. Shah, R. Nativio, S. L. Berger, Epigenetic mechanisms of longevity and aging. *Cell* **166**, 822–839 (2016).
32. Y. F. Liu *et al*., ICAM-1 deficiency in the bone marrow niche impairs quiescence and Repopulation of hematopoietic stem cells. *Stem Cell Reports* **11**, 258–273 (2018).
33. A. Wilson *et al*., c-Myc controls the balance between hematopoietic stem cell self-renewal and differentiation. *Genes Dev.* **18**, 2747–2763 (2004).
34. C. J. Poole, J. van Riggelen, MYC-master regulator of the cancer epigenome and transcriptome. *Genes (Basel)* **8**, 142 (2017).
35. J. van Riggelen, A. Yetil, D. W. Felsher, MYC as a regulator of ribosome biogenesis and protein synthesis. *Nat. Rev. Cancer* **10**, 301–309 (2010).
36. F. Radtke *et al*., Deficient T cell fate specification in mice with an induced inactivation of Notch1. *Immunity* **10**, 547–558 (1999).
37. J. E. Delmore *et al*., BET bromodomain inhibition as a therapeutic strategy to target c-Myc. *Cell* **146**, 904–917 (2011).
38. C. Y. Lin *et al*., Transcriptional amplification in tumor cells with elevated c-Myc. *Cell* **151**, 56–67 (2012).
39. S. de Pretis *et al*., Integrative analysis of RNA polymerase II and transcriptional dynamics upon MYC activation. *Genome Res.* **27**, 1658–1664 (2017).
40. A. Baluapuri *et al*., MYC recruits SPT5 to RNA polymerase II to promote processive transcription elongation. *Mol. Cell* **74**, 674–687e611 (2019).
41. S. Kinoshita *et al*., Cyclin-dependent kinase 9 as a potential specific molecular target in NK-cell leukemia/lymphoma. *Haematologica* **103**, 2059–2068 (2018).
42. M. L. Truitt, D. Ruggero, New frontiers in translational control of the cancer genome. *Nat. Rev. Cancer* **16**, 288–304 (2016).
43. A. J. Waskiewicz, A. Flynn, C. G. Proud, J. A. Cooper, Mitogen-activated protein kinases activate the serine/threonine kinases Mnk1 and Mnk2. *EMBO J.* **16**, 1909–1920 (1997).
44. N. L. Korneeva, A. Song, H. Gram, M. A. Edens, R. E. Rhoads, Inhibition of mitogen-activated protein kinase (MAPK)-interacting kinase (MNK) preferentially affects translation of mRNAs containing both a 5′-terminal cap and hairpin. *J. Biol. Chem.* **291**, 3455–3467 (2016).
45. P. P. Roux, I. Topisirovic, Signaling pathways involved in the regulation of mRNA translation. *Mol. Cell. Biol.* **38**, e00070-18 (2018).
46. M. Grzmil *et al*., MAP kinase-interacting kinase 1 regulates SMAD2-dependent TGF-β signaling pathway in human glioblastoma. *Cancer Res.* **71**, 2392–2402 (2011).
47. A. Bianchini *et al*., Phosphorylation of eIF4E by MNKs supports protein synthesis, cell cycle progression and proliferation in prostate cancer cells. *Carcinogenesis* **29**, 2279–2288 (2008).
48. C. R. Bramham, K. B. Jensen, C. G. Proud, Tuning specific translation in cancer metastasis and synaptic memory: Control at the MNK-eIF4E Axis. *Trends Biochem. Sci.* **41**, 847–858 (2016).
49. T. P. Herbert, G. R. Kilhams, I. H. Batty, C. G. Proud, Distinct signalling pathways mediate insulin and phorbol ester-stimulated eukaryotic initiation factor 4F assembly and protein synthesis in HEK 293 cells. *J. Biol. Chem.* **275**, 11249–11256 (2000).
50. U. Knauf, C. Tschopp, H. Gram, Negative regulation of protein translation by mitogen-activated protein kinase-interacting kinases 1 and 2. *Mol. Cell. Biol.* **21**, 5500–5511 (2001).
51. M. Kesarwani *et al*., Targeting c-FOS and DUSP1 abrogates intrinsic resistance to tyrosine-kinase inhibitor therapy in BCR-ABL-induced leukemia. *Nat. Med.* **23**, 472–482 (2017).
52. T. B. Campbell, S. Basu, G. Hangoc, W. Tao, H. E. Broxmeyer, Overexpression of Rheb2 enhances mouse hematopoietic progenitor cell growth while impairing stem cell repopulation. *Blood* **114**, 3392–3401 (2009).
53. M. P. Creyghton *et al*., Histone H3K27ac separates active from poised enhancers and predicts developmental state. *Proc. Natl. Acad. Sci. U.S.A.* **107**, 21931–21936 (2010).
54. S. Heinz, C. E. Romanoski, C. Benner, C. K. Glass, The selection and function of cell type-specific enhancers. *Nat. Rev. Mol. Cell Biol.* **16**, 144–154 (2015).
55. H. Santos-Rosa *et al*., Active genes are tri-methylated at K4 of histone H3. *Nature* **419**, 407–411 (2002).
56. Y. Zhang *et al*., Coordinated regulation of protein synthesis and degradation by mTORC1. *Nature* **513**, 440–443 (2014).
57. L. Jossé, J. Xie, C. G. Proud, C. M. Smales, mTORC1 signalling and eIF4E/4E-BP1 translation initiation factor stoichiometry influence recombinant protein productivity from GS-CHOK1 cells. *Biochem. J.* **473**, 4651–4664 (2016).
58. S. K. Tasian, D. T. Teachey, S. R. Rheingold, Targeting the PI3K/mTOR pathway in pediatric hematologic malignancies. *Front. Oncol.* **4**, 108 (2014).
59. J. Polivka, Jr, F. Janku, Molecular targets for cancer therapy in the PI3K/AKT/mTOR pathway. *Pharmacol. Ther.* **142**, 164–175 (2014).
60. F. Chiarini, C. Evangelisti, G. Lattanzi, J. A. McCubrey, A. M. Martelli, Advances in understanding the mechanisms of evasive and innate resistance to mTOR inhibition in cancer cells. *Biochim. Biophys. Acta Mol. Cell Res.* **1866**, 1322–1337 (2019).
61. Y. G. Gangloff *et al*., Disruption of the mouse mTOR gene leads to early post-implantation lethality and prohibits embryonic stem cell development. *Mol. Cell. Biol.* **24**, 9508–9516 (2004).
62. A. Trumpp *et al*., c-Myc regulates mammalian body size by controlling cell number but not cell size. *Nature* **414**, 768–773 (2001).
63. X. Cai *et al*., Runx1 deficiency decreases ribosome biogenesis and confers stress resistance to hematopoietic stem and progenitor cells. *Cell Stem Cell* **17**, 165–177 (2015).

Downloaded at Palestinian Territory, occupied on December 11, 2021

www.manaraa.com